University of Texas Rio Grande Valley

ScholarWorks @ UTRGV

Physics and Astronomy Faculty Publications and Presentations

College of Sciences

1-1-2000

The HÎ² index as an age indicator of old stellar systems: The effects of horizontal-branch stars

Hyun Chul Lee

Suk Jin Yoon

Young Wook Lee

Follow this and additional works at: https://scholarworks.utrgv.edu/pa_fac

 Part of the Astrophysics and Astronomy Commons

Recommended Citation

Hyun Chul Lee, et. al., (2000) The HÎ² index as an age indicator of old stellar systems: The effects of horizontal-branch stars.Astronomical Journal120:2998. DOI: http://doi.org/10.1086/301471

This Article is brought to you for free and open access by the College of Sciences at ScholarWorks @ UTRGV. It has been accepted for inclusion in Physics and Astronomy Faculty Publications and Presentations by an authorized administrator of ScholarWorks @ UTRGV. For more information, please contact justin.white@utrgv.edu, william.flores01@utrgv.edu.

THE ASTRONOMICAL JOURNAL, 120:998–1005, 2000 August
© 2000. The American Astronomical Society. All rights reserved. Printed in U.S.A.

THE Hβ INDEX AS AN AGE INDICATOR OF OLD STELLAR SYSTEMS: THE EFFECTS OF HORIZONTAL-BRANCH STARS

HYUN-CHUL LEE, SUK-JIN YOON, AND YOUNG-WOOK LEE
Center for Space Astrophysics and Department of Astronomy, Yonsei University, Shinchon 134, Seoul 120-749, Korea;
hclee@csa.yonsei.ac.kr, sjyoon@csa.yonsei.ac.kr, ywlee@csa.yonsei.ac.kr
Received 2000 March 15; accepted 2000 April 17

ABSTRACT

The strength of the Hβ index is computed for the integrated spectra of model globular clusters from the evolutionary population synthesis. For the first time, these models take into account the detailed systematic variation of horizontal-branch (HB) morphology with age and metallicity. Our models show that the Hβ index is significantly affected by the presence of blue HB stars. Because of the contribution from blue HB stars, the Hβ does not monotonically decrease as metallicity increases at a given age. Instead, it reaches a maximum strength when the distribution of HB stars is centered around 9500 K, the temperature at which the Hβ index becomes strongest. Our models indicate that the strength of the Hβ index increases as much as 0.75 Å because of the presence of blue HB stars. The comparison of the recent Keck observations of the globular cluster system in the Milky Way with those in the giant elliptical galaxies NGC 1399 and M87 shows a systematic shift in the Hβ-metallicity plane. Our models suggest that this systematic difference is explained if the mean age of globular cluster systems in giant elliptical galaxies is several billion years older than the Galactic counterpart. Further observations of globular cluster systems in the external galaxies from the large ground-based telescopes and space UV facilities will enable us to clarify whether this difference is indeed due to the age difference or whether other explanations are also possible.

Key words: galaxies: formation — galaxies: star clusters — stars: horizontal-branch

1. INTRODUCTION

For distant stellar populations, one relies upon integrated colors or spectra to investigate their ages and metallicities since individual stars are not resolved. In this paper, we will focus on the Hβ index, which is widely used as an age indicator. It has been highlighted because (1) it is the only index that shows the anticorrelation with metallicity and (2) it is sensitive to temperature, reaching a maximum strength at around 9500 K (Worthey 1994).

Most of the previous works (e.g., Worthey 1994; Buzzoni 1995), however, have been done on the assumption that stars near the main-sequence turnoff (MSTO) region are the most dominant sources for the integrated strength of Hβ. Consequently, without meticulous consideration for stars beyond the red giant branch (RGB), they claimed that the strength of Hβ depends on the location of the MSTO, which in turn depends on the age at a given metallicity. Several investigators, however, have cast some doubt upon the sensitivity of the Hβ index given the presence of other warm stars, especially blue horizontal-branch (HB) stars (see, e.g., Rabin 1982; Christian & Schommer 1983; Burstein et al. 1984; Buzzoni, Mantegazza, & Gariboldi 1994; de Freitas Pacheco & Barbuy 1995; Ferguson 1995; Fisher, Franx, & Illingworth 1995; Bressan, Chiosi, & Tantalo 1996; Lee, Lee, & Park 1996; Greggio 1997; Jorgensen 1997).

On the observational side, it was barely possible to obtain low signal-to-noise (S/N) spectra of globular clusters in systems outside the Local Group (e.g., Mould, Oke, & Nemec 1987; Mould et al. 1990; Huchra & Brodie 1987; Brodie & Huchra 1991; Grillmair et al. 1994). These spectra have been used only for kinematic information. With the advent of 10 m–class telescopes, however, Kissler-Patig et al. (1998) and Cohen, Blakeslee, & Ryzhov (1998) have successfully obtained relatively high S/N spectra that provide reliable line index calibration for globular clusters in NGC 1399 and M87, the central giant elliptical galaxies in the Fornax and Virgo clusters. Figure 1 shows the distribution of globular clusters in the Milky Way and of those in NGC 1399 in the Hβ-Mg_2 plane. At first glance, there seems to be little difference between these two systems, especially considering the large uncertainties in the NGC 1399 globular cluster system. Careful scrutiny of the data, however, indicates a systematic difference in that the metal-rich clusters in NGC 1399 have higher Hβ compared with their Galactic counterparts, while the opposite seems to be the case for the more metal-poor clusters. In fact, a Kolmogorov-Smirnov test yields only a 2.14% probability that the two samples, excluding the two very metal-rich NGC 1399 clusters, are extracted from the same parent population.

This systematic difference has motivated us to explore the sensitivity of the integrated Hβ strength with detailed population synthesis models that reproduce the systematic variation of HB morphology with age and metallicity. The HB stars are not unusual components of old stellar systems since they are ubiquitously found from the color-magnitude diagrams (CMDs) of Galactic globular clusters and the stellar evolution theories reproduce them remarkably (e.g., Lee, Demarque, & Zinn 1990, 1994). In § 2, our population models developed with and without consideration for HB stars are presented. Section 3 reinforces the validity of our models with HB stars by comparing them with a sample of Galactic globular clusters, and it compares our results with the observations of globular cluster systems in the Milky Way, M31, NGC 1399, and M87. Finally, § 4 discusses major implications from our work.

2. POPULATION MODELS WITH AND WITHOUT HORIZONTAL-BRANCH STARS

The present models were constructed by using our evolu-

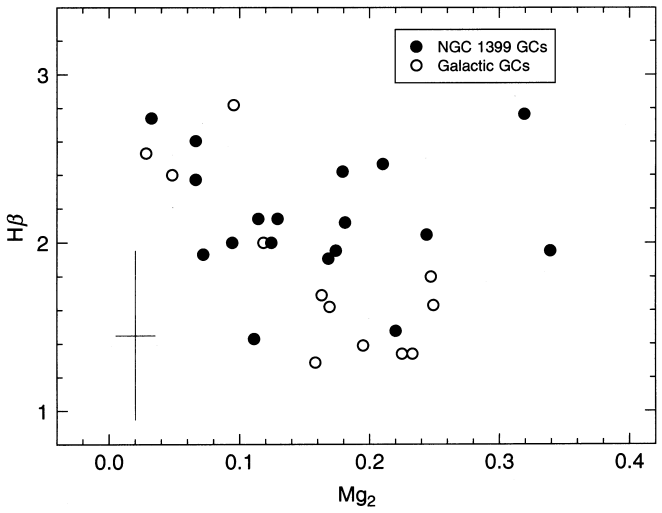

FIG. 1.—Comparison of Galactic globular clusters (*open circles*; data from Cohen, Blakeslee, & Ryzhov 1998) with those in NGC 1399 (*filled circles*; data from Kissler-Patig et al. 1998) in the Hβ-Mg_2 plane. Observational errors are displayed for clusters in NGC 1399.

tionary population synthesis code, which was developed to study the stellar populations in globular clusters. For our population models, the Yale Isochrones (Demarque et al. 1996), rescaled for α-element enhancement (Salaris, Chieffi, & Straniero 1993), and the HB evolutionary tracks by Yi, Demarque, & Kim (1997) have been used. For metal-rich ([Fe/H] > −0.5) populations, the value of the helium enrichment parameter, $\Delta Y/\Delta Z = 2$, is assumed (cf. Maeder 1992; Pagel et al. 1992). The Salpeter (1955) initial mass function (IMF),

$$dN = CM^{-\chi}dM\ , \tag{1}$$

with $\chi = 2.35$, is adopted for the relative number of stars along the isochrones, but the effects of the variations of χ are also tested and described in section 2.2. For the conversion from theoretical quantities to observable quantities, we have taken the most recently compiled stellar library of Lejeune, Cuisinier, & Buser (1998) to cover the largest possible ranges in stellar parameters, such as metallicity, temperature, and gravity.

The strength of the spectral line index is calculated by using either

$$\mathrm{EW} = \Delta\lambda[1 - (F_\lambda/F_C)]\ , \tag{2}$$

or

$$\mathrm{Mag} = -2.5\ \log\ (F_\lambda/F_C)\ , \tag{3}$$

where $\Delta\lambda$ is an index bandpass and F_λ and F_C are the fluxes in the index bandpass and the pseudocontinuum flux in the index bandpass, respectively (Worthey et al. 1994). First, for each star (or bunch of stars after binning) with a given metallicity, temperature, and gravity, we find the flux values at both pseudocontinuum regions for each index from the stellar library. Then we calibrate F_C at the center of each index bandpass. Second, we calculate either the equivalent width (EW; for Hβ and Mg *b*) or the magnitude (Mag; for Mg_2) using the fitting functions of Worthey et al. (1994). Then we solve for F_λ. Finally, after F_C and F_λ are all summed up for a simple stellar population of a given metallicity and age, we compute the integrated strengths of spectral line indexes by using formulae (2) and (3). Table 1 lists the Lick/IDS system bandpasses that have been used in this work as defined in Burstein et al. (1984). Unless otherwise noted, we have used Burstein et al. (1984) definitions in this work to be compatible with the data that we fitted in Section 3.

We have not taken into account either blue stragglers (BSs) or post-HB stars in our models, since it is hard to quantify them systematically with metallicity and age because of poor knowledge about their evolution and also because of their scarcity. With the inclusion of the BSs, we would expect the strength of Hβ to slightly increase. We suspect, however, that the post-HB stars would hardly affect this index, mainly because of their paucity.

2.1. *Population Models without Horizontal-Branch Stars*

Before proceeding to the construction of models with HB stars, without considering HB stars we compared our models with those of Worthey (1994), the most widely used models, to make sure that our calculations are consistent with those of previous investigations. For this purpose, we have taken the same index bandpasses that Worthey (1994) used in his model calculations. It is clear from Figure 2 that these models generate very similar results, although there are slight differences, mostly due to the different isochrones employed. It is also worth noting that Worthey models that treat HB stars as red clumps are similar to our models without HB stars, as already noted by Rabin (1982; cf. Worthey & Ottaviani 1997; see the caption of their Fig. 6). One can see from Figure 2 that without the systematic variation of HB morphology that we employ in the following subsection, the Hβ decreases as metallicity and age increase simply because the MSTO temperature decreases with these variations.

Recently there have been an increasing number of reports that the evolutionary timescale from main sequence (MS) to RGB should be substantially decreased if developments in the stellar evolution theories, particularly those due to the effects of diffusion and the Coulomb correction on the equation of state in the isochrones, are applied (see, e.g., Chaboyer et al. 1996; Salaris, Degl'Innocenti, & Weiss 1997; Cassisi et al. 1998). In particular, according to Chaboyer et al. (1996), it is suggested that the age of Galactic globular clusters should be reduced by 18% after one considers this improved input physics. Hence, a correction was applied in

TABLE 1

DEFINITIONS FOR SPECTRAL LINE INDEXES

Index	Blue Continuum (Å)	Feature Bandpass (Å)	Red Continuum (Å)	Type
Hβ	4829.50–4848.25	4849.50–4877.00	4878.25–4892.00	EW
Mg_2.....	4897.00–4958.25	5156.00–5197.25	5303.00–5366.75	Mag
Mg *b*.....	5144.50–5162.00	5162.00–5193.25	5193.25–5207.00	EW

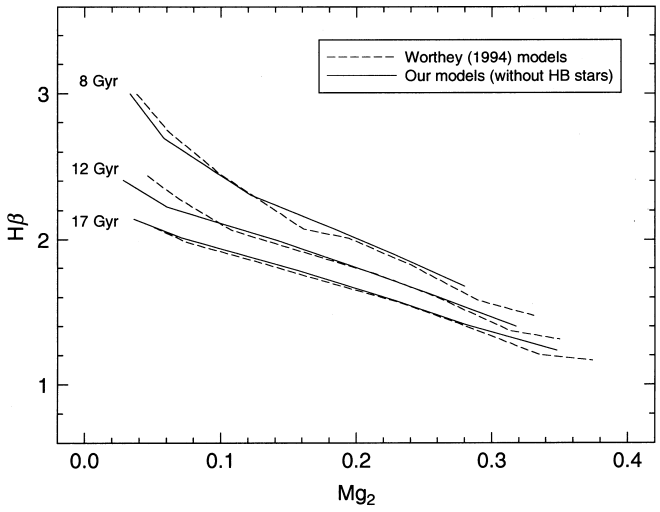

FIG. 2.— Hβ strengths from our models without HB stars (*solid lines*) compared with those from Worthey (1994) models (*dashed lines*) as a function of metallicity (Mg_2) for ages 8, 12, and 17 Gyr. Note that the two models generate very similar results.

our models to simulate these age-reduction effects. For example, 15 Gyr isochrones are employed to represent 12 Gyr populations. One can see this effect on the Hβ index in Figure 3. The dashed lines were plotted using the standard Yale isochrones, while the solid lines show what we described above after employing the correction. It is clear from Figure 3 that the isochrones with the improved input physics (*solid lines*) should result in a decrease in Hβ, mainly because of the decrease of the MSTO temperature. Hereafter, these simulated isochrones are used for further computations even though the conclusions drawn below should be relatively insensitive to this correction. Furthermore, it should be noted that only relative ages in this study are meaningful until isochrones that incorporate an input physics that is fully consistent with real stars emerge.

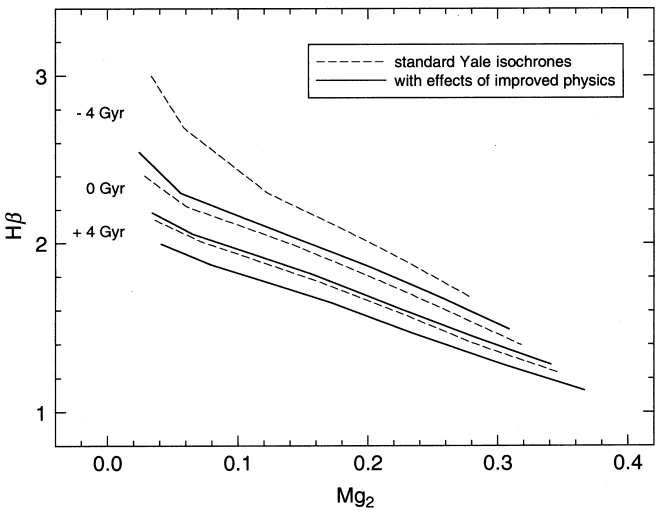

FIG. 3.—Similar to Fig. 2, but with the standard Yale isochrones (*dashed lines*) systematically shifted to simulate the effects of recent improvements in input physics in the stellar models (see text). The line labeled "$\Delta t = 0$ Gyr" corresponds to 12 Gyr populations and the lines labeled "-4 Gyr" and "$+4$ Gyr" indicate populations 4 Gyr younger and 4 Gyr older, respectively.

2.2. *Population Models with Horizontal-Branch Stars*

To include HB stars in our models, first, we need to estimate the amounts of mass loss on the RGB. In this study, we have adopted Reimers's mass-loss relation (Reimers 1975). The value of η, the empirical fitting factor in Reimers's mass-loss relation, was estimated by matching the tight correlations between [Fe/H] and HB morphology type [$(B-R)/(B+V+R)$; Lee et al. 1994] for the inner halo Galactic globular clusters (Galactocentric radius ≤ 8 kpc; Fig. 4, *filled circles and squares*). The value of $\eta = 0.65$ was determined at their recently favored mean age (~ 12 Gyr, $\Delta t = 0$ Gyr) in the light of a new distance scale suggested by *Hipparcos* data (e.g., Feast & Catchpole 1997; Gratton et al. 1997; Reid 1998; Chaboyer et al. 1998), as well as from recent developments of stellar evolution theories (Chaboyer et al. 1996; Salaris & Weiss 1997; Cassisi et al. 1999). The modified Gaussian mass distribution,

$$\Psi(M) = \Psi_0[M - (\overline{M_{\rm HB}} - \Delta M)](M_{\rm RG} - M) \times \exp\left[-\frac{(\overline{M_{\rm HB}} - M)^2}{2\sigma^2}\right], \quad (4)$$

where σ is a mass dispersion factor in solar masses, Ψ_0 is a normalization factor, and $\overline{M_{HB}}$ ($\equiv M_{\rm RG} - \Delta M$) is the mean mass of HB stars (Lee et al. 1990; Demarque et al. 2000), was employed with $\sigma = 0.02\,M_\odot$.

Figure 4 presents our model isochrones in the plot of the HB type as a function of [Fe/H]. Figure 5 vividly shows

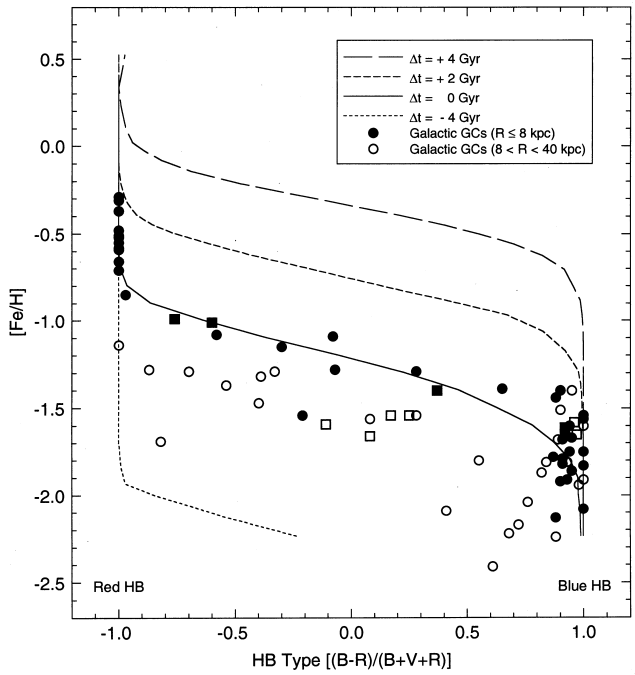

FIG. 4.—Value $\eta = 0.65$, the empirical fitting factor in Reimers's mass-loss relation, estimated by matching the tight correlations between [Fe/H] and the HB morphology type of the inner halo Galactic globular clusters (Galactocentric radius ≤ 8 kpc; *filled symbols*) at their currently favored mean age (~ 12 Gyr, $\Delta t = 0$ Gyr; *solid line*). Open circles and squares represent the outer halo Galactic globular clusters. The dotted line represents the predicted model relationship for the population that is 4 Gyr younger than the inner halo Galactic globular clusters, while the short-dashed and long-dashed lines represent those for the populations that are 2 and 4 Gyr older, respectively, than the inner halo Galactic globular clusters. Squares are the selected Galactic globular clusters from Burstein et al. (1984) that are compared with models in Fig. 7. Data are from Lee, Demarque, & Zinn (1994).

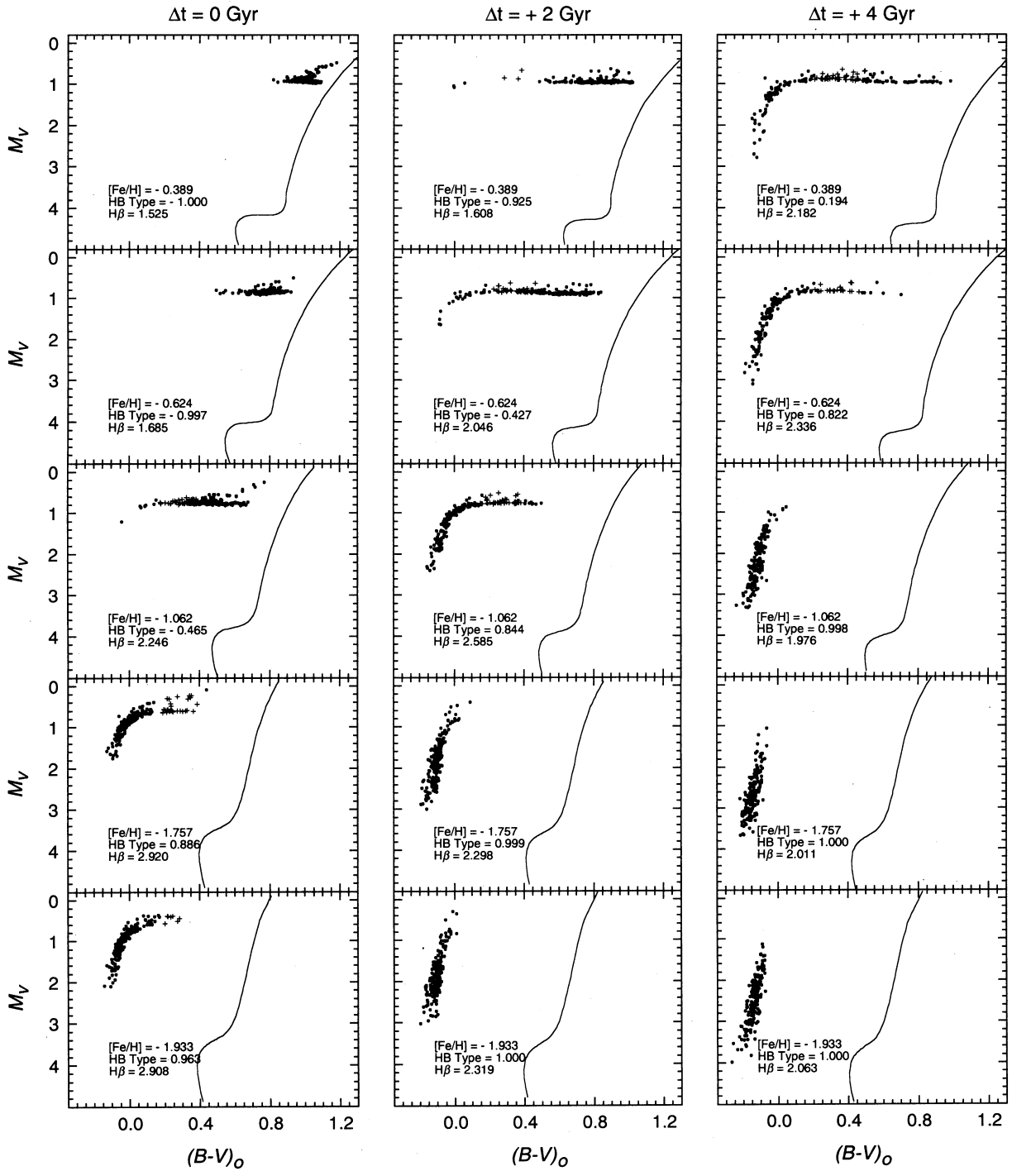

FIG. 5.—Selected synthetic CMDs at three different ages defined in Figure 4. At each age, five CMDs are shown, arranged according to decreasing metallicity. Solid lines represent the corresponding isochrones from MS to RGB to indicate the variations of the MSTO. Both the HB morphology type $[(B-R)/(B+V+R)]$ and the strength of Hβ are given in each set of CMDs. RR Lyrae stars are denoted by crosses. Note that the strength of Hβ depends not only on the location of the MSTO but also on the distribution of HB stars.

how the isochrones in Figure 4 are generated. From the CMDs in the left column of Figure 5, one clearly sees the effect of metallicity, the first parameter that governs the HB morphology type, in that HB becomes redder as metallicity increases. By reading Figure 5 horizontally, one can also see that age works as the global second parameter that characterizes the HB morphology in that it becomes bluer with increasing age at a given metallicity (see also Lee et al. 1994).

In Figure 6, the variations of Hβ strength as a function of metallicity are plotted for four ages based on the model loci of Figure 4. Note that, unlike the models without HB stars (*dashed lines*), distinct wavelike features appear in our models with HB stars (*solid lines*). These features are clearly understood with the aid of Figure 5. For example, by referring to the five CMDs in the left column of Figure 5 from bottom to top and by following the model line of $\Delta t = 0$ Gyr in Figure 6 from low to high metallicity, it is evident

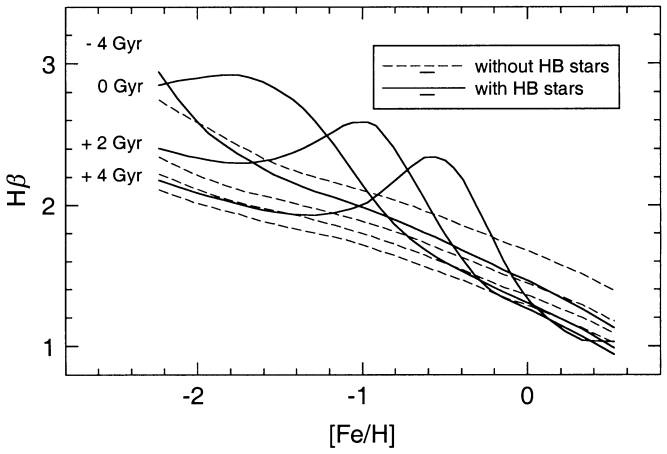

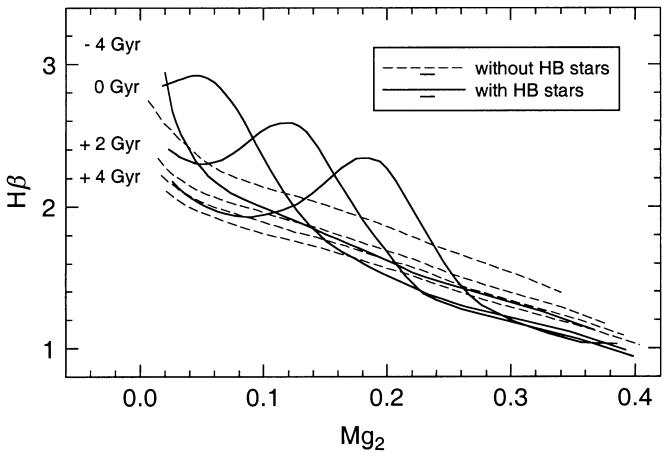

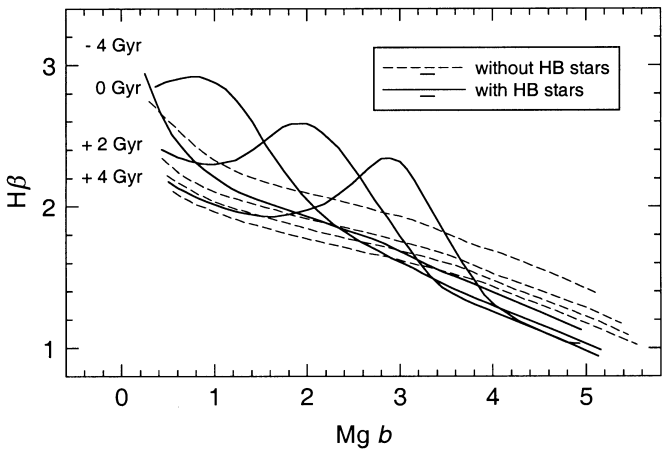

FIG. 6.—Effect of HB stars on the strength of Hβ as predicted from our models. The strength of Hβ is plotted against [Fe/H] (*top*), Mg_2 (*middle*), and Mg *b* (*bottom*) for four relative ages ($\Delta t = -4$, 0, +2, and +4 Gyr, respectively). Dashed lines represent models without HB stars, while solid lines represent those with HB stars based on the model loci of Figure 4 (see text).

that (1) there is an enhancement in Hβ and it becomes a maximum where HB stars are centered about 9500 K [$(B-V)_0 \sim 0$], the temperature at which the Hβ index becomes strongest, even though the temperature of MSTO is getting lower with increasing metallicity, (2) after the peak, the Hβ enhancement decreases since the mean temperature of HB stars is getting lower, and (3) with only cool red HB stars, the strength of Hβ becomes even slightly more weak than that in the models without HB stars. In addition, it should be noted that the peak of the Hβ enhancement moves to higher metallicity as age increases.

Therefore, the strength of Hβ does not simply decrease with either increasing age or increasing metallicity when HB stars are included in the models. As Figure 5 clearly demonstrates, the strength of Hβ depends not only on the location of the MSTO but also on the distribution of HB stars. Now it is clear that the blue HB stars around $(B-V)_0 \sim 0$ are the key contributors to the strength of Hβ. The differences in Hβ strengths between the models with and without HB stars are as much as 0.75 Å at the peak. This is in accordance with the empirical estimate by Burstein et al. (1984) and Buzzoni et al. (1994), although these authors did not investigate the systematic variations we report here.

It must be noted here that the fitting functions of Worthey et al. (1994) are given to only 13,260 K. For stars hotter than 13,260 K, we extrapolated their fitting functions for Mg_2 and Mg *b*. For Hβ, however, we employed tables by Kurucz (1993) that give explicit values for the Balmer line strengths at a given metallicity, temperature, and gravity. A systematic shift ($\sim$6.1 Å) was necessary to make Hβ values from Kurucz (1993) match those from the fitting function of Worthey et al. (1994) at about 13,000 K. Note that this treatment is applied only to blue HB stars from very metal-poor and very old populations (the left side of the peaks for model lines of $\Delta t = +2$ and +4 Gyr in Fig. 6). Therefore, the general wavelike features, including the location of peaks, should not be affected by this treatment. The fitting functions in this temperature range are needed in the near future, however, to better estimate the effects from those hot stars on the spectral line indexes.

We also have looked into the dependence of strengths of Hβ and Mg_2 on the initial mass function. It is found that the variations of the exponent χ of the initial mass function between 1.35 and 3.35 are negligible in that they correspond roughly to the errors estimated from the fitting functions, $\sim$0.22 Å for Hβ and $\sim$0.008 mag for Mg_2.

3. COMPARISON WITH OBSERVATIONS

3.1. *Test of the Models via Galactic Globular Clusters*

The remarkable effects of HB stars on the strength of Hβ are elaborated in the previous section. To corroborate our results, our models with HB stars are tested using observations of Galactic globular clusters, the only objects that the independent HB morphology types can be evaluated. We have chosen a sample within a narrow range of metallicity, so that the metallicity effects on the HB morphology can be put aside. Then we investigate whether the strengths of Hβ of the sample globular clusters are really related to their HB morphology.

In Figure 7, we have fixed the metallicity ([Fe/H] = −1.535; *dashed lines* and −0.814; *solid lines*) and calculated the strengths of Hβ at varying ages. As age increases, the MSTO temperature is getting lower, while the HB morphology becomes bluer. It is shown here that the strength of Hβ gradually increases as the HB morphology becomes bluer, surpassing the MSTO temperature variations. The thin lines, which actually have nothing to do with HB types, only indicate the level of Hβ strengths without HB stars.

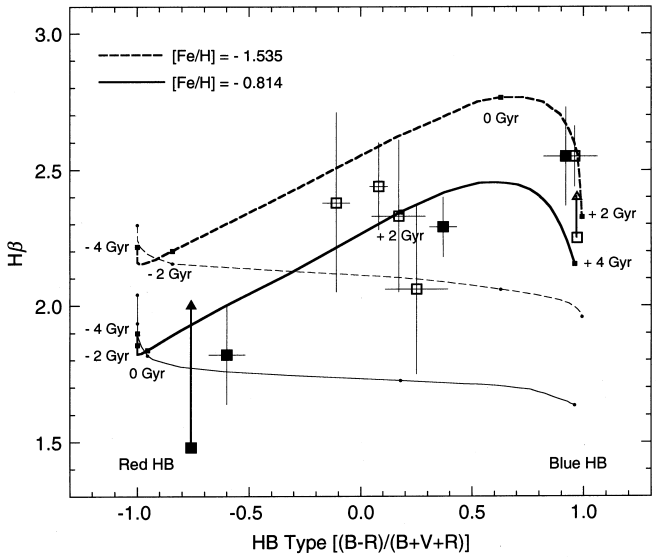

FIG. 7.—Variations of Hβ strength with HB morphology at given metallicity. In the model calculations (*thick lines*), the age is varied from young to old (*left to right*) to generate various types of HB morphology. The thin lines indicate the level of Hβ strengths without HB stars. A sample of Galactic globular clusters within the similar metallicity range is superposed here. Filled and open squares are same as in Fig. 4. Two clusters (NGC 6171; *filled triangle* and M13; *open triangle*) also obtained with the Keck telescope by Cohen et al. (1998), are connected to Burstein et al. (1984) data by straight lines. Note that with the systematic variation of HB morphology our models trace the observational data reasonably well.

The sample of Galactic globular clusters within the similar metallicity range (data from Burstein et al. 1984), which are denoted by squares in Figure 4, is superposed. It is clear from Figure 7 that (1) the inclusion of relevant HB stars is essential in the population models for Hβ and (2) our assumption of age as the global second parameter reproduces the observations within the errors.

What is evident from this test is that the inclusion of pertinent HB stars predominates over the MSTO temperature variations for the strengths of Hβ in globular clusters. Therefore, in the construction of population synthesis models for old stellar systems such as globular clusters, one should take great care about HB stars.

3.2. *Comparison with Globular Cluster Systems*

Having confirmed that the detailed modeling of HB is crucial in the use of the Hβ index as an age indicator, we now compare our results with observations of globular cluster systems in the Milky Way, M31, NGC 1399, and M87. It is important to note here that all of these observations except those for M31 globular clusters were carried out at the Keck telescope with the identical instrumental configuration, the Low Resolution Imaging Spectrograph (Oke, de Zeeuw, & Nemec 1995), so that the comparisons between these cluster systems are not affected by systematic and instrumental inhomogeneity.

First, Figure 8*a* presents the comparison of the globular cluster system in the Milky Way with that in M31 in the Hβ-Mg_2 plane. For the Galactic globular cluster system, a set of 12 globular clusters obtained by Cohen et al. (1998) are used. For that in M31, 15 of 18 globular clusters in common with Burstein et al. (1984) and Huchra et al. (1996)

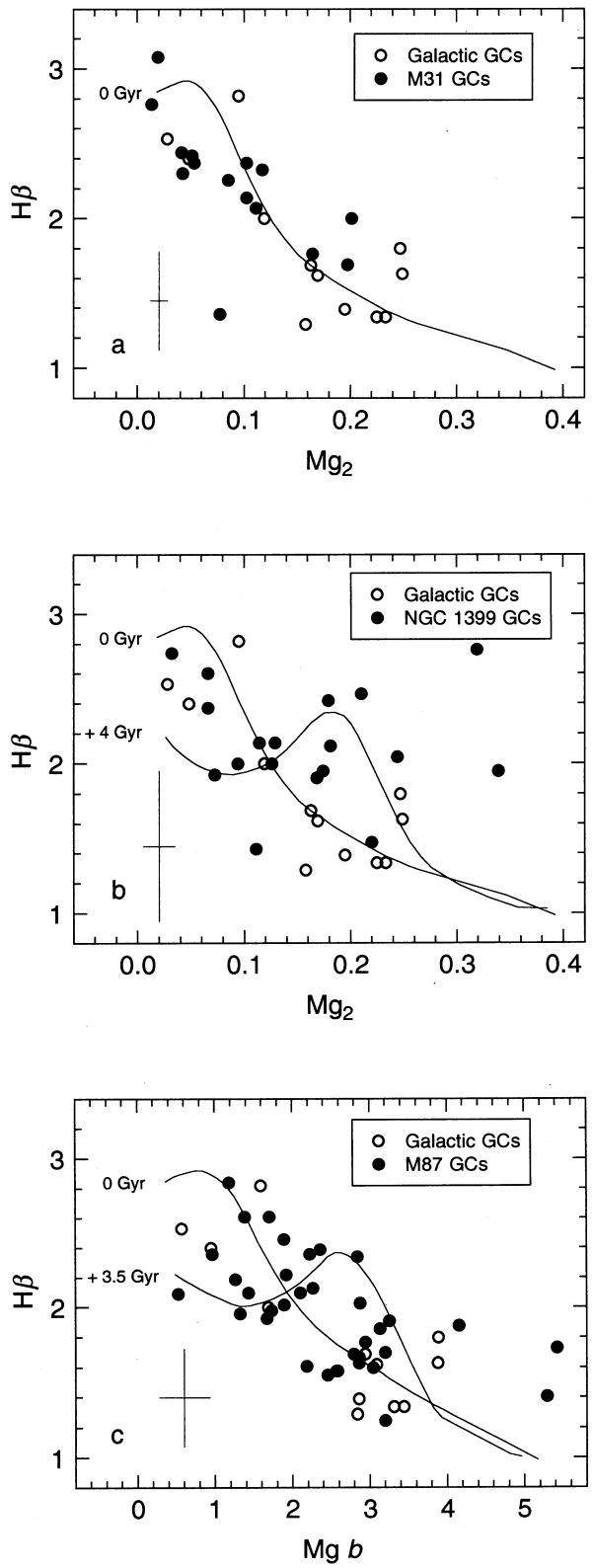

FIG. 8.—Globular cluster system in the Milky Way compared with (*a*) that in M31 and (*b*) that in NGC 1399 in the Hβ-Mg_2 plane and compared with (*c*) that in M87 in an Hβ-Mg *b* plane. All of the observations except those for M31 globular clusters were made with the Keck telescope using an identical instrumental configuration (see text). Our models with HB stars are overlaid. Note that the overall distributions of the globular cluster systems in NGC 1399 and M87 are different from those in the Milky Way and M31, indicating that the giant ellipticals may contain globular clusters whose mean age is several billion years older than the ages of those in the Milky Way.

are used. We have taken Huchra et al. (1996) data here, since they were obtained with higher resolution and high S/N at the Multiple Mirror Telescope. Three clusters (G1, G33, and G222; G from Sargent et al. 1977) are excluded because they show more than 1 Å differences in Hβ between Burstein et al. (1984) and Huchra et al. (1996) observations. The errors given in the figure are the average from the M31 sample. It is found from Figure 8*a* that the two globular cluster systems are fundamentally not quite different, in terms of Hβ strength as a function of metallicity. They are reasonably well traced by our models for $\Delta t = 0$ Gyr, i.e., $t = 12$ Gyr.

Next, in Figure 8*b*, the globular cluster system in NGC 1399 is compared with that in the Milky Way. Despite the still large observational uncertainties in the NGC 1399 globular cluster system obtained by Kissler-Patig et al. (1998), the systematic shift that we noticed in §1 between these two systems is now explained by the age difference. Figure 8*b* implies that the mean age of the NGC 1399 globular cluster system is perhaps systematically older than its Galactic counterpart by about 4 Gyr.

In Figure 8*c*, we compare the M87 globular cluster system with that in the Milky Way. For M87 globular clusters, the Hβ-Mg *b* plane is used, since Cohen et al. (1998) preferred the narrower Mg *b* index to the broader Mg_2 index because of their observational condition. From 150 sample globular clusters in Cohen et al. (1998), we have taken 35 that have relatively high S/N (QSNR > 50). It appears from Figure 8*c* that the age difference of $\Delta t = +3.5$ Gyr best reproduces the M87 globular cluster system in the Hβ-Mg *b* plane, although better data are clearly needed to confirm this.

We do not claim here that all of the globular clusters in giant elliptical galaxies are coeval and older than their Galactic counterparts. In fact, there is now a growing body of evidence that suggests age variations among globular clusters in the Milky Way (e.g., Lee et al. 1994; Sarajedini, Chaboyer, & Demarque 1997). In this respect, we suspect that there would be similar age variations among globular clusters in giant elliptical galaxies. However, the quality of the present data, even taken with the 10 m–class telescope, is still far from being capable of attempting such detailed analysis.

4. DISCUSSION

We have found in this work that (1) the integrated Hβ strengths of old stellar systems, such as globular clusters, are significantly affected by HB stars and (2) the present observational data for the globular cluster systems are best understood in terms of systematic age differences among them in that globular clusters in more massive galaxies are older. If our age estimate is confirmed, this would indicate that the star formation in denser environments has proceeded much more rapidly and efficiently, so that the initial epoch of star formation in more massive (and denser) systems occurred several billion years earlier than that of the Milky Way (see also Lee 1992). It is of considerable interest, in this respect, to find that a similar age difference is inferred from the "metal-poor HB solution" of the UV upturn phenomenon of local giant elliptical galaxies (Park & Lee 1997; Yi et al. 1999). The above solution suggests that the dominant UV sources in elliptical galaxies are very old, hot metal-poor HB stars and their post-HB progeny, although metal-rich post–asymptotic giant branch (PAGB) stars also contribute some UV flux. In this picture, nearby giant elliptical galaxies are about 3 Gyr older than the Milky Way. This is also consistent with the view that a substantial population of the massive early-type galaxies formed earlier at very high redshift (e.g., Larson 1990; Maoz 1990; Bender, Ziegler, & Bruzual 1996; Harris, Harris, & McLaughlin 1998; Stanford, Eisenhardt, & Dickinson 1998).

Further observations of globular cluster systems in nearby galaxies from the large ground-based telescopes are imperative to elucidate this possible systematic age difference. In addition, satellite UV photometry could also provide a test for the validity of our results presented in this paper, because it is expected that older globular clusters would reveal the stronger UV fluxes and the bluer UV colors because their blue HB stars should be hotter than those in the Galactic counterparts at a given metallicity (see Fig. 1 of Park & Lee 1997). These new observations, together with the detailed population models presented here, will undoubtedly help to clarify our understanding of the formation epoch of galaxies.

Support for this work was provided by the Creative Research Initiatives Program of the Korean Ministry of Science and Technology.

REFERENCES

Bender, R., Ziegler, B., & Bruzual, G. 1996, ApJ, 463, L51
Bressan, A., Chiosi, C., & Tantalo, R. 1996, A&A, 311, 425
Brodie, J. P., & Huchra, J. P. 1991, ApJ, 379, 157
Burstein, D., Faber, S. M., Gaskell, C. M., & Krumm, N. 1984, ApJ, 287, 586
Buzzoni, A. 1995, ApJS, 98, 69
Buzzoni, A., Mantegazza, L., & Gariboldi, G. 1994, AJ, 107, 513
Cassisi, S., Castellani, V., Degl'Innocenti, S., Salaris, M., & Weiss, A. 1999, A&AS, 134, 103
Cassisi, S., Castellani, V., Degl'Innocenti, S., & Weiss, A. 1998, A&AS, 129, 267
Chaboyer, B., Demarque, P., Kernan, P. J., & Krauss, L. M. 1998, ApJ, 494, 96
Chaboyer, B., Demarque, P., Kernan, P. J., Krauss, L. M., & Sarajedini, A. 1996, MNRAS, 283, 683
Christian, C. A., & Schommer, R. A. 1983, ApJ, 275, 92
Cohen, J. G., Blakeslee, J. P., & Ryzhov, A. 1998, ApJ, 496, 808
de Freitas Pacheco, J. A., & Barbuy, B. 1995, A&A, 302, 718
Demarque, P., Chaboyer, B., Guenther, D., Pinsonneault, M., & Yi, S. 1996, Yale Isochrones (New Haven: Yale Univ. Obs.)
Demarque, P., Zinn, R., Lee, Y.-W., & Yi, S. 2000, AJ, 119, 1398
Feast, M. W., & Catchpole, R. M. 1997, MNRAS, 286, L1
Ferguson, H. C. 1995, in IAU Symp. 164, Stellar Populations, ed. P. C. van der Kruit & G. Gilmore (Dordrecht: Kluwer), 239
Fisher, D., Franx, M., & Illingworth, G. 1995, ApJ, 448, 119
Gratton, R. G., Fusi Pecci, F., Carretta, E., Clementini, G., Corsi, C. E., & Lattanzi, M. 1997, ApJ, 491, 749
Greggio, L. 1997, MNRAS, 285, 151
Grillmair, C. J., Freeman, K. C., Bicknell, G. V., Carter, D., Couch, W. J., Sommer-Larsen, J., & Taylor, K. 1994, ApJ, 422, L9
Harris, W. E., Harris, G. L. H., & Mclaughlin, D. E. 1998, AJ, 115, 1801
Huchra, J. P., & Brodie, J. P. 1987, AJ, 93, 779
Huchra, J. P., Brodie, J. P., Caldwell, N., Christian, C., & Schommer, R. 1996, ApJS, 102, 29
Jorgensen, I. 1997, MNRAS, 288, 161
Kissler-Patig, M., Brodie, J. P., Schroder, L. L., Forbes, D. A., Grillmair, C. J., & Huchra, J. P. 1998, AJ, 115, 105
Kurucz, R. L. 1993, ATLAS9 Stellar Atmosphere Programs and 2 km/s Grid (Cambridge: Smithsonian Astrophys. Obs.)
Larson, R. B. 1990, PASP, 102, 709

Lee, H.-C., Lee, Y.-W., & Park, J.-H. 1996, J. Korean Astron. Soc., 29, S133
Lee, Y.-W. 1992, PASP, 104, 798
Lee, Y.-W., Demarque, P., & Zinn, R. 1990, ApJ, 350, 155
———. 1994, ApJ, 423, 248
Lejeune, T., Cuisinier, F., & Buser, R. 1998, A&AS, 130, 65
Maeder, A. 1992, A&A, 264, 105
Maoz, E. 1990, ApJ, 359, 257
Mould, J. R., Oke, J. B., de Zeeuw, P. T., & Nemec, J. M. 1990, AJ, 99, 1823
Mould, J. R., Oke, J. B., & Nemec, J. M. 1987, AJ, 92, 53
Oke, J. B., de Zeeuw, P. T., & Nemec, J. M. 1995, PASP, 99, 1823
Pagel, B. E. J., Simonson, E. A., Terlevich, R. J., & Edmunds, M. G. 1992, MNRAS, 255, 325
Park, J.-H., & Lee, Y.-W. 1997, ApJ, 476, 28
Rabin, D. 1982, ApJ, 261, 85
Reid, I. N. 1998, AJ, 115, 204
Reimers, D. 1975, Mem. Soc. R. Sci. Liège, 8, 369
Salaris, M., Chieffi, A., & Straniero, O. 1993, ApJ, 414, 580
Salaris, M., Degl'Innocenti, S., & Weiss, A. 1997, ApJ, 479, 665
Salaris, M., & Weiss, A. 1997, A&A, 327, 107
Salpeter, E. E. 1955, ApJ, 121, 161
Sarajedini, A., Chaboyer, B., & Demarque, P. 1997, PASP, 109, 1321
Sargent, W. L. W., Kowal, C. T., Hartwick, F. D. A., & van den Bergh, S. 1977, AJ, 82, 947
Stanford, S. A., Eisenhardt, P. R., & Dickinson, M. 1998, ApJ, 492, 461
Worthey, G. 1994, ApJS, 95, 107
Worthey, G., Faber, S. M., Gonzalez, J. J., & Burstein, D. 1994, ApJS, 94, 687
Worthey, G., & Ottaviani, D. L. 1997, ApJS, 111, 377
Yi, S., Demarque, P., & Kim, Y.-C. 1997, ApJ, 482, 677
Yi, S., Lee, Y.-W., Woo, J.-H., Park, J.-H., Demarque, P., & Oemler, A., Jr. 1999, ApJ, 513, 128